Scattering Analysis of High Performance Large Sandwich Radomes

Reuven Shavit, *Senior Member, IEEE,* Adam P. Smolski, Eric Michielssen and Raj Mittra, *Fellow, IEEE*

Abstract—**Typically, large radar antennas are covered with radomes in order to protect them from weather conditions and to enable them to operate continuously without loss of precision. Due to their large size, the radomes are assembled from many panels connected together forming joints or seams. In many applications the panels are type-A sandwiches that are optimized for minimum transmission loss over moderately narrow bandwidths. The seams and joints in a sandwich radome introduce scattering effects that can degrade the overall electromagnetic performance of the radome. Tuning the dielectric seams with conductive wires and optimizing their geometry is, therefore, crucial to enhancing the electromagnetic performance of the radome. This paper addresses the problem of systematically tuning the dielectric seams and presents both numerical and experimental results to illustrate the tuning procedure. Also included in the paper are results showing the effect of the tuning of the radome on the radiation pattern of an enclosed aperture of circular or elliptic shape.**

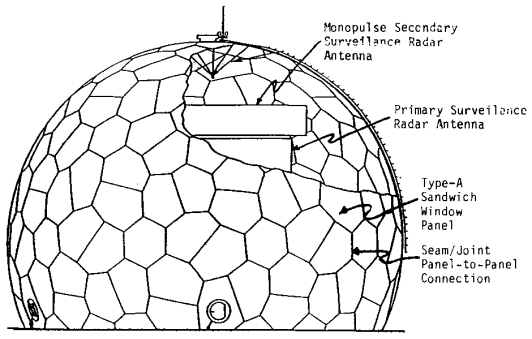

Fig. 1. Sandwich radome geometry.

Introduction

THE common shape of large radomes is a spherical dome as shown in Fig. 1. This shape is chosen not only because of structural and manufacturing considerations, but also because it provides symmetry during the antenna scanning. For moderately narrow bandwidths and high transmissivity (95%), the radome can be a type-A sandwich panel construction with dielectric panel-to-panel seam connections. The radome is constructed from many panels with a quasi-radome geometry to reduce the cumulative effect of scattering from the seams. The degree of randomness of the seam geometry can increase as the seam length decreases. However, such a decrease in the seam length also has associated negative effects, e.g., increase in the total blockage due to the seams and decrease in the cost effectiveness of the panel manufacturing process. Consequently, there is a trade-off issue to be considered in the use of randomness in the design of radomes.

The physical dimensions of the seams are usually determined by structural considerations, such as maximum wind speed and the resultant stresses the seams have to sustain. Without electromagnetic consideration, however, radome seams may degrade the total system performance by introducing high scattering levels. The reduction of the scattering effect from the seams can be obtained by introducing conductive wires in the dielectric seams. The conductive currents induced in the wires can be designed to partially offset the effects of polarization currents induced in the dielectric seam and thereby produce a net reduction of the scattering effect.

The scattering analysis from such a tuned dielectric seam with parallel (transverse magnetic (TM) case) and perpendicular (transverse electric (TE) case) conductive wires/strips to the seam axis have been addressed in the literature. Most of the investigators of the TM case [1]–[4] have employed the electric field integral equation (EFIE) volume integral equation in conjunction with the method of moments (MM) and have regarded the scattering from the seam to be equivalent to the superposition of the scattering from a multifilament structure confined in the cross section of the seam. The TE case of a dielectric seam tuned with conductive strips perpendicular to its axis has been analyzed by Michielssen and Mittra [5] using the spectral domain formulation and an MM solution.

The analysis of the total scattering effect from all the seams in front of the antenna's aperture is similar to that described by Kay [6] for metal space frame radomes. Both Kay [6] and Chang [7] considered a circular aperture enclosed in the radome illuminating the seams with a collimated beam. This approach is valid only for relatively large apertures (in wavelengths) enclosed in the radome. We will extend the analysis to the case of elliptical apertures and will include the divergence effects of small or asymmetrical antennas enclosed in the radome. Finally, we will present computed

Manuscript received October 2, 1990; revised July 12, 1991.

R. Shavit and A. P. Smolski are with Electronic Space Systems Corp., Concord, MA 01742-4697.

E. Michielssen and R. Mittra are with the Electromagnetic Communication Laboratory, Department of Electrical Engineering, University of Illinois, Urbana, IL 61801.

IEEE Log Number 9105946.

results which show the importance of the randomness in the seam geometry on the antenna pattern.

II. Tuning a Single Seam

The reduction of the radome scattering effect or improvement in the radome transmissivity can be obtained by minimizing the scattering level from the individual seams. Depending on the incident field polarization, both vertical (TM case) and horizontal (TE case) polarization currents will be induced in the seam. The magnitude of those currents increase with frequency, therefore, it is crucial to offset those currents for high performance radome applications at microwave frequencies. Fig. 2 shows the tuning mechanism with vertical and horizontal conductive strips.

The basic parameters which determine the performance of a seam are the induced field ratio (IFR) and the seam's scattering pattern. The IFR concept was introduced by Kennedy [8] to characterize scattering from cylinders and was used extensively by Rusch *et al.* [9] and Ruze [10] to analyze the scattering from reflector antenna struts. The IFR is the ratio of the scattered field by the seam to the field radiated by the geometrical shadow area of the seam containing that incident field.

Using the Michielssen and Mittra [4] formulation we have computed the IFR dependence with frequency for a dielectric seam of rectangular cross section with dimensions 2 in × 4 in. The IFR dependence of a tuned and an untuned seam is shown in Fig. 3. The electrical properties of the seam are $\epsilon_r = 4.6$ and $\tan\delta = 0.014$. The seam is tuned with a grid of conductive strips located on its center line, spaced 0.277 in apart and with a strip width of 0.062 in. The data presented is for the TM case and at normal ($\phi = 0$) incidence. The computed data is compared to the measured data.

At the tuning frequency 5.6 GHz the magnitude of the IFR drops significantly compared to that of the untuned seam. In addition, the IFR phase goes through the 180 degree value close to the tuning frequency, a feature common to resonant devices.

Fig. 4 shows the field distribution amplitude and phase in the tuned and untuned seam cross section. At the locations of the strips the total electric field goes to zero. Moreover, the phase of the electric field is more uniform compared to that of the untuned seam. The uniformity of the phase distribution is a good indicator of the transparency of the seam because it resembles the uniform phase front of the incident field.

Fig. 5 shows the comparison between the computed scattering pattern of the untuned and tuned dielectric seam. One can observe the significant reduction of the scattering levels in the forward direction compared to that of the untuned seam.

The seam's IFR of two adjacent sandwich panels was measured by moving two type-A sandwich panels with a seam in between on a track in front of a pair of receiving and transmitting horns. The amplitude and phase of the receiving signal throughout the panel movement were recorded. Typical recorded signals (amplitude and phase) for both the parallel (TM case) and perpendicular (TE case) polarizations are shown in Fig. 6. One should notice the reference signal

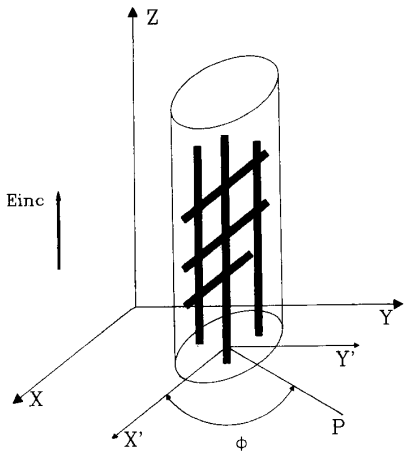

Fig. 2. Basic geometry of a dielectric slab with tuning grid.

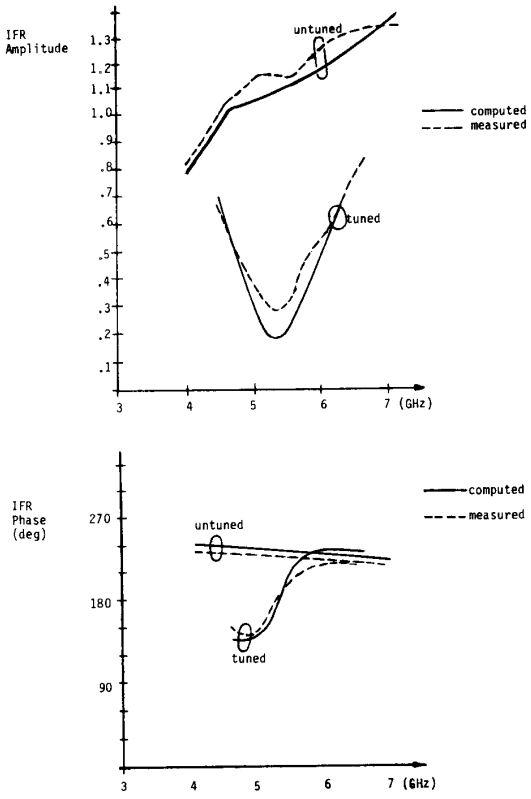

Fig. 3. IFR versus frequency for a tuned/untuned dielectric slab 2 in × 0.4 in (TM case) at normal incidence.

before the panels cross the boresight line between the horns, the diffraction effect when the panels begin to cross this line, the insertion phase delay (IPD) and the insertion loss of the panel and the phase and amplitude perturbation in the seam area. The recorded signal is symmetric with respect to the seam axis. The perturbation of the amplitude and phase in the seam region is significantly reduced for the tuned case.

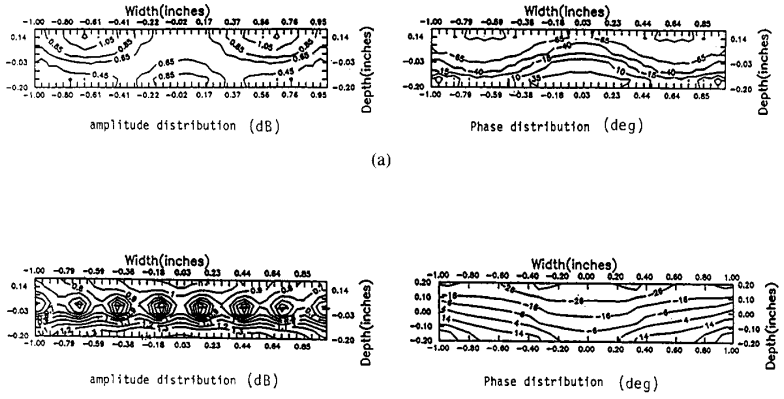

Fig. 4. Field distribution in a tuned and untuned dielectric slab at the tuning frequency (5.6 GHz) at normal incidence. (a) Untuned. (b) Tuned.

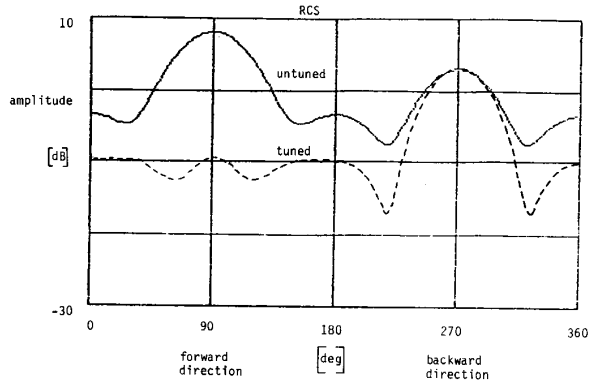

Fig. 5. Calculated scattering pattern for tuned and untuned dielectric slab 2 in × 0.4 in (TM case) at 5.6 GHz.

Based on the measured phase and amplitude perturbation in the seam region, one can compute the IFR of the seam using the following formula [9]:

$$\text{IFR} = \left(10^{0.05\Delta\alpha}e^{j\Delta\Phi} - 1\right)\frac{e^{-j45^\circ}}{W}\sqrt{\frac{\lambda\eta_0\eta_0'}{\eta_0 + \eta_0'}} \qquad (1)$$

where

$\Delta\alpha$(dB)	amplitude change due to the tested seam in the forward direction
$\Delta\phi$ (degree)	phase change due to the tested seam in the forward direction
W	the width of the shadow area of the seam's geometrical cross section on the incident wavefront
λ	wavelength
η_0'	distance between the tested seam and the transmitting horn
η_0	distance between the tested seam and the receiving horn

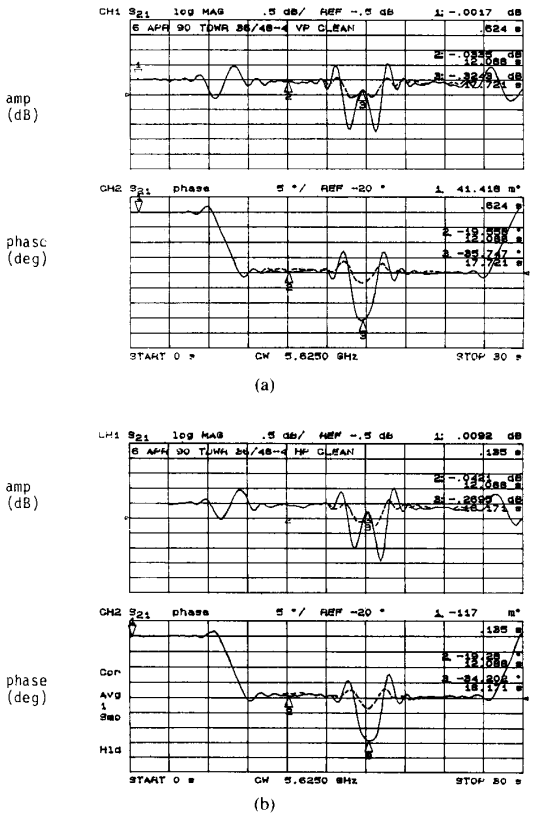

Fig. 6. Recorded signals (throughout the panel movement for tuned (----) and untuned (——) seams at 5.625 GHz. (a) Vertical polarization (TM case). (b) Horizontal polarization (TE case).

III. Scattering Analysis of the Seams

Fig. 7 shows a schematic diagram of the scattering mechanism from the seams. For increased generality, the aperture of the antenna is chosen to be of elliptical shape with its major axes $2a \times 2b$ and its center offset from the radome

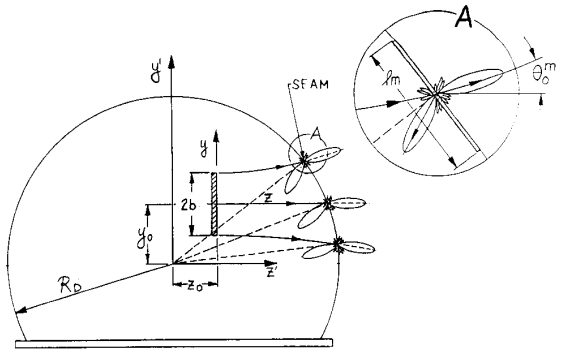

Fig. 7. The geometry of the radome and the scattering mechanism.

center (y_0, z_0). Due to the divergence effect of the antenna's radiation beam, the incident angle on the mth seam and its peak scattering angle is (θ_0^m, ϕ_0^m). The coordinate system for the scattering analysis is shown in Fig. 7. To determine the perturbation due to the seam scattering we compute initially the unperturbed far-field pattern of the antenna enclosed in the radome. In our analysis we have assumed that the aperture distribution $f(x, y)$ [11] of the antenna's elliptical aperture is

$$f(x, y) = C + 1(1 - C)\left[1 - \frac{x^2}{a^2} - \frac{y^2}{b^2}\right]^p \tag{2}$$

where C is the pedestal illumination and p is an exponential factor which determines the shape of the aperture distribution. Given the aperture distribution $f(x, y)$ one can compute the far field pattern $F(\theta, \phi)$ [11]

$$F(\theta, \phi) = \int_{-a}^{a}\int_{-b}^{b} f(x', y') e^{jk(x' \sin\theta \cos\phi + y' \sin\theta \sin\phi)}\, dx'\, dy'. \tag{3}$$

Substitution of (2) into (3) and introduction of a new set of variables (r, ϕ') in place of (x', y') via the equations

$$\begin{aligned} x' &= ar \cos\phi' \\ y' &= ar \cos\alpha \sin\phi' \end{aligned} \tag{4}$$

where $\cos\alpha = b/a$, yields a closed-form expression for the far field from an elliptical aperture

$$F(\theta, \phi) = \pi a^2 \cos\alpha \left[C\frac{2J_1(u)}{u} + (1 - C)\frac{2^{p+1}\Gamma(p + 1) J_{(p+1)}(u)}{u^{p+1}} \right] \tag{5}$$

in which $J_p(U)$ is the Bessel function of pth order, $\Gamma(p + 1)$ is the Gamma function, and

$$u = ka \sin\theta \left(1 - \sin^2\phi \sin^2\alpha\right)^{1/2}. \tag{6}$$

To evaluate the incident field upon the seams we have assumed that the radiated near field from the elliptical aperture can be approximated by a Gaussian beam [12] with two independent waists $W_{el}(z)$ and $W_{az}(z)$ in elevation and azimuth, respectively. In general, the waist $W(z)$ is given by [12],

$$W(z) = W_0\left[1 + \left(\lambda z/\pi W_0^2\right)^2\right]^{1/2} \tag{7}$$

where W_0 is the Gaussian beam waist at $z = 0$ and it can be either $W_{0,el}$ (elevation) or $W_{0,az}$ (azimuth). We have computed W_0 by equating the actual 3 dB beamwidth of the aperture to the 3 dB beamwidth of the Gaussian beam approximation. The radius of curvature $R(z)$ of the Gaussian beam is given by [12]

$$R(z) = z\left[1 + \left(\pi W_0^2/\lambda z\right)^2\right] \tag{8}$$

and there are two radii of curvature, viz., R_{az} and R_{el} in azimuth and elevation, respectively. Given $W(z)$ and $R(z)$ one can compute the field intensity $f(x, y, z)$ of the Gaussian beam at any distance (z) from the antenna's aperture,

$$f(x, y, z) = \left[\frac{W_{0,el}W_{0,az}}{W_{el}W_{az}}\right]^{1/2} e^{-\frac{x^2}{w_{az}^2} - \frac{y^2}{w_{el}^2}} \cdot e^{-jkz_e - j\frac{\pi}{\lambda}\left(\frac{x^2}{R_{az}} + \frac{y^2}{R_{el}}\right)} e^{j\tan^{-1}\left(\frac{\lambda z}{\pi w_{0,el} w_{0,az}}\right)}. \tag{9}$$

One can observe that the intensity of the electric field decays exponentially transverse to its propagation axis. The intensity of the Gaussian beam drops by more than 30 dB at a lateral distance of $4W_{az} \times 4W_{el}$. In view of this, we have ignored in our calculations the scattering effect from the seams beyond this distance and have designated the aperture $4W_{az} \times 4W_{el}$ as the effective illuminated antenna aperture. Let the coordinates of the mth seam center of the radome be (x_m, y_m, z_m), and let this seam be projected on the effective illuminated antenna aperture. Let the angle of inclination of the projected seam with respect to the y axis be δ_m. The peak of the scattering pattern from the mth joint is determined by the incident angle (θ_0^m, ϕ_0^m) of the corresponding constituent ray of the Gaussian beam at its center as shown in Fig. 7. In the derivation, we have used the coordinate systems (θ, ϕ) in which θ is the elevation angle measured from the $x - z$ plane and ϕ is the azimuthal angle measured from the z axis and confined to the $x - z$ plane.

For the purpose of computing the scattering from the seams, we have assumed that the field radiated by the mth seam is equivalent to that from a straight current strip with length l_m, width W_m and with a constant transverse and axial current distribution. This is a valid approximation for the purposes of computing the radiation field. An alternative would be to consider the actual scattering pattern from the tuned seam on an individual basis; however, this approach significantly complicates the computation. Using the approximation mentioned above, the far-field scattering pattern $I_m(\theta, \phi)$ from the mth seam is written as

$$I_m(\theta, \phi) = W_m l_m \frac{\sin A_m}{A_m} \frac{\sin B_m}{B_m} e^{jk(x_m u_m + y_m v_m + z_m d_m)} \tag{10}$$

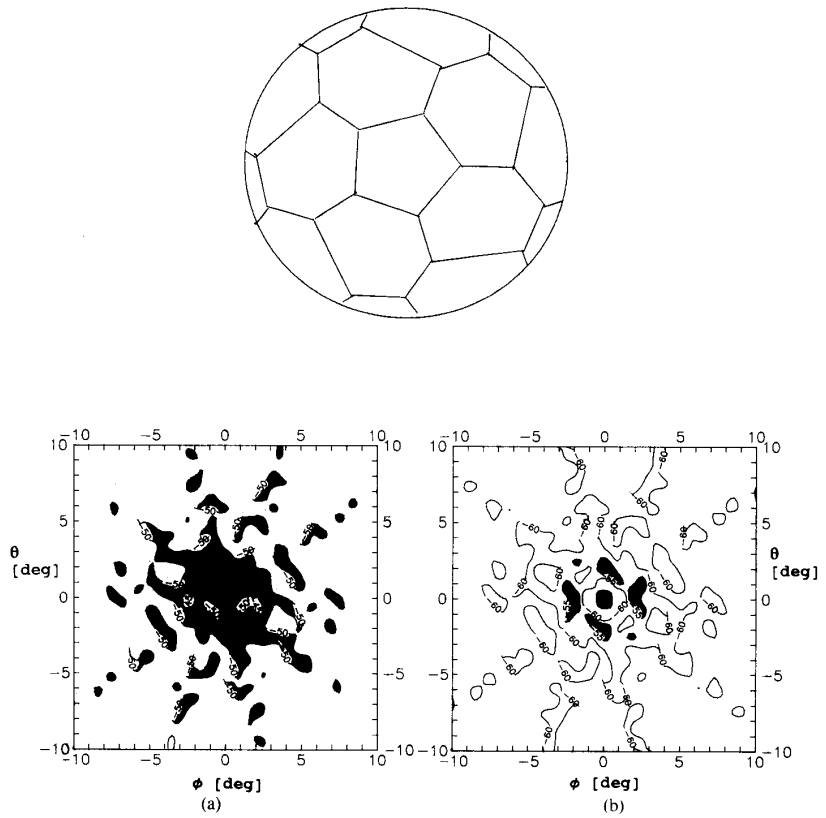

Fig. 8. Comparison between the scattering patterns from a randomized geometry with (a) untuned and (b) tuned seams.

where

$$u_m = \cos(\theta, \theta_0^m)\sin(\phi, \phi_0^m)$$

$$v_m = \sin(\theta, \theta_0^m)$$

$$d_m = \cos(\theta, \theta_0^m)\cos(\phi, \phi_0^m) \tag{11}$$

and

$$A_m = \frac{kW_m}{2}\sin\theta'\cos(\phi' + \delta_m) \tag{12}$$

$$B_m = \frac{kl_m}{2}\sin\theta'\sin(\phi' + \delta_m) \tag{13}$$

$$\sin\theta' = \left[\sin^2(\theta - \theta_0^m) + \cos^2(\theta - \theta_0^m)\sin^2(\phi - \phi_0^m)\right]^{1/2} \tag{14}$$

$$\sin\theta' = \frac{\sin(\theta - \theta_0^m)}{\sin\theta'}. \tag{15}$$

The scattering from the seams is weighted by the illumination function $f(x_m, y_m, z_m)$ given by (9), and proportional to the IFR and the scattering pattern $I_m(\theta, \phi)$ given by (10). Thus the total scattered field from M seams can be computed by

$$F_s(\theta, \phi) = \sum_{m-1}^{M} g_m I_m(\theta, \phi/\theta_0^m, \phi_0^m) f_m(x_m, y_m, z_m) \tag{16}$$

in which [7]

$$g_m = g_\parallel \cos^2\delta_m + g_\perp \sin^2\delta_m \tag{17}$$

$g_\parallel$, $g_\perp$ are the parallel and perpendicular components of the IFR of the seam. Given that the unperturbed pattern of the antenna is $F(\theta, \phi)$ as given by (5) and the scattered pattern from the seams is $F_s(\theta, \phi)$ as given by (16), one can compute the perturbed pattern $F'(\theta, \phi)$ from

$$F'(\theta, \phi) = F(\theta, \phi) + F_s(\theta, \phi). \tag{18}$$

Fig. 8 shows a typical projection of a randomized radome geometry on a 25 ft diameter aperture operating at 5.6 GHz (vertical polarization). A comparison is presented between the scattering patterns for untuned and tuned seams. The seams are 4 in wide with the untuned seam IFR equal to $-0.4 - j0.022$ while the tuned seam IFR is equal to $-0.16 + j0$. One can observe the reduction (approximately 15 dB) in the scattering level in the tuned case. In both cases, the

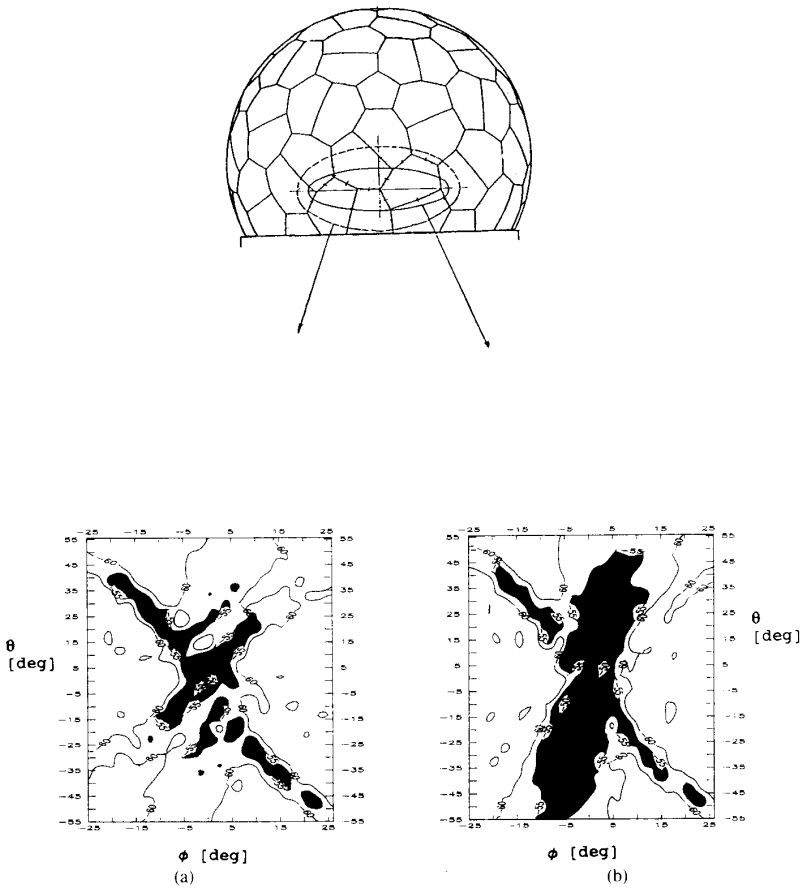

Fig. 9. Comparison between the scattering patterns of the seams with and without the divergence effect. (a) Aperture with divergence effect (29.7 ft × 13.1 ft). (b) Aperture without divergence effect (27 ft × 5.8 ft).

scattered energy is uniformly distributed in space due to the randomized geometry of the radome.

As an example of the beam spreading effect on the scattering pattern of the seams, we have considered a passive array 27 ft × 5.8 ft operating at 1.09 GHz with vertical polarization enclosed in a 56 ft tuned sandwich radome. In the computation we have assumed that the tapering over the aperture is 15 dB with $p = 2$. The parallel polarization IFR is $-0.013 + j.013$ and the perpendicular polarization IFR is $-0.12 + j.001$ with a seam width of 4 in. Due to Gaussian beam spreading, the illuminated aperture on the radome surface is 29.7 ft × 13.1 ft, which indicates that more seams are illuminated than evident from the 27 ft × 5.8 ft aperture projection. Fig. 9 shows the comparison between the computed scattering patterns with and without the inclusion of the divergence effect of the radiating aperture. One can observe that the divergence causes a reduction of approximately 5 dB at the peak of the scattered energy and a more uniform distribution over a wider sector. This result can be explained by the quadratic phase error introduced in the illumination of the seams located over the spherical surface of the radome compared to the almost uniform illumination if this effect is neglected. In addition, the total transmission loss (with illumination divergence) from the radome improves from 0.06 dB to 0.02 dB.

IV. Geometry Optimization

In many radar applications, and especially those which involve low sidelobes, it is important to reduce the scattering effect due to the radome in a specified solid angle (θ, ϕ). In the previous sections, we have shown how this task can be accomplished by tuning the seams and quantifying the scattering level. The next step would be to optimize the seam geometry. The basic parameters which characterize the scattering effect are the peak of the scattered energy level and its distribution in space. The peak scattering level is proportional to the total length of the seam and its IFR. We have reduced the IFR by tuning the seams. The next step is to reduce the total seam length while maintaining a high degree of randomness. Although this approach reduces the total seam blockage which is beneficial from the aspect of the transmission loss, it increases the size of the panels, which may or may not be desirable from a manufacturing or installation point of view. Continuing to increase the individ-

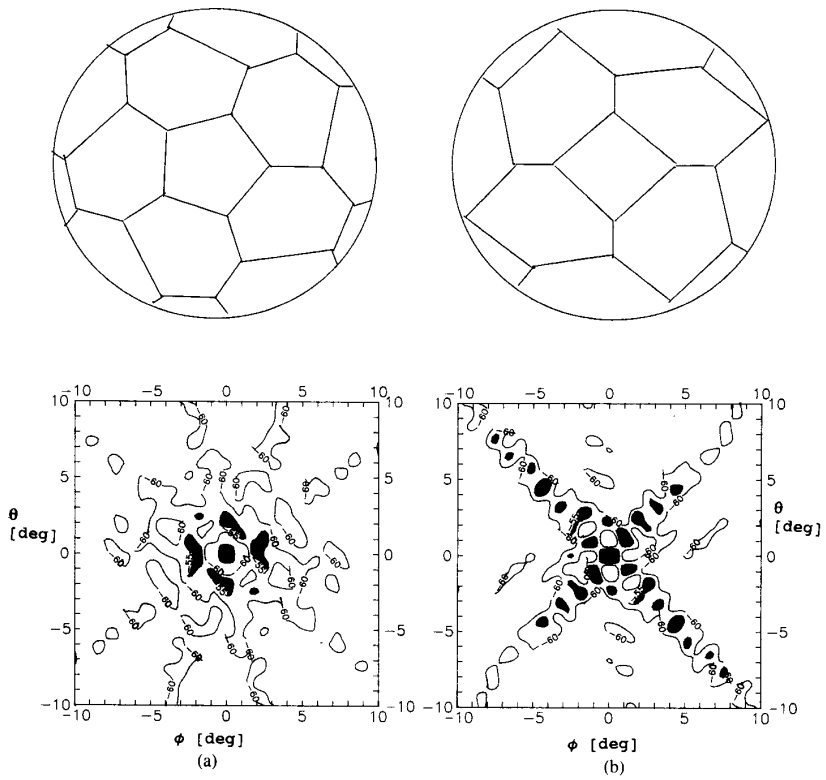

Fig. 10. Comparison between (a) a randomized and (b) a regular geometry and their scattering patterns.

ual seam lengths will decrease the randomness or increase the array factor. Both effects have negative implications on the scattering distribution. Fig. 10 shows a comparison between the scattering patterns from a typical seam geometry with a low blockage and a low degree of randomness and a randomized geometry. The seams are projected on a 25 ft diameter reflector antenna and the scattering patterns are computed at 5.625 GHz with both parallel and perpendicular tuned seam IFR's. One can observe that for the regular geometry on the $\pm 45°$ planes the scattering level is significantly higher than in other planes. This pattern has an undesirable distribution of the scattered energy. On the other hand, for the randomized geometry, the scattered energy is seen to be more uniformly distributed.

Another factor to be considered in the design is the variation of the projected seam geometry on the antenna aperture as the antenna scans in azimuth and elevation. A qualitative parameter of this effect is the variation of the seam blockage for different antenna aspect angles. For a "good" geometry, the blockage varies mildly with antenna aspect angle.

V. Conclusion

In the design of large sandwich radomes, scattering effects from the seams play an important role. To obtain a high performance radome, one should consider both reducing the scattering from the individual seams and optimizing the seam geometry. The calculated data backed by experimental results show that with proper tuning of the seams with conductive strips one can significantly reduce the IFR of the individual seams and improve their scattering pattern. In the scattering analysis, we have demonstrated the importance of including in the divergence effect of the beam of the radiating antenna, especially for small antennas. The presented results also show how an increase in the "geometrical randomness" makes the scattering effect from the seams more uniform.

Acknowledgment

The authors wish to express their thanks to Al Cohen for his encouragement and stimulating discussions in the course of this work.

References

[1] K. C. Chang and A. P. Smolski, "The effect of impedance matched radomes on SSR antenna systems," in *IEEE Conf. Proc. Radar 87*, London, U.K., Oct. 1987, pp. 155–159.

[2] F. C. Smith, B. Chambers, and J. C. Bennett, "Improvement in the electrical performance of dielectric space frame radomes by wire loading," in *IEEE Conf. Antennas Propagat.*, ICAP 89, Coventry, U.K., Apr. 1989, pp. 530–534.

[3] J. H. Richmond, "Scattering by a dielectric cylinder of arbitrary cross-section shape," *IEEE Trans. Antennas Propagat.*, vol. AP-13, pp. 334–341, May 1965.

[4] E. Michielssen and R. Mittra, "RCS reduction of dielectric cylinders using a simulated annealing approach," in *Symp. Dig. IEEE Conf. Antennas Propagat.*, Dallas, TX, May 1990, pp. 1268–1271.

[5] ____, "TE plane wave scattering by a dielectric cylinder loaded with perfectly conducting strips," in *Symp. Dig. IEEE Conf. Antennas Propagat.*, Dallas, TX, May 1990, p. 125.

[6] A. F. Kay, "Electrical design of metal space frame radomes," *IEEE Trans. Antennas Propagat.*, vol. AP-13, pp. 188-202, Mar. 1965.
[7] K. C. Chang and A. P. Smolski, "A radome for air traffic control SSR radar systems," in *IEEE Int. Conf. Radar 87*, Oct. 1987, pp. 155-159.
[8] P. D. Kennedy, "An analysis of the electrical characteristics of structurally supported radomes," Ohio State Univ. Rep. under Contract AF-30 (602)-1620, Nov. 1958.
[9] W. V. T. Rusch, J. A. Hansen, C. A. Klein, and R. Mittra, "Forward scattering from square cylinders in the resonance region with application to aperture blockage," *IEEE Trans. Antennas Propagat.*, vol. AP-24, pp. 182-189, Mar. 1976.
[10] J. Ruze, "Feed support blockage loss in parabolic antennas," *Microwave J.*, vol. 11, no. 12, 1968.
[11] S. Cornbleet, *Microwave Optics*. London, U.K.: Academic, 1976.
[12] P. F. Goldsmith, "Quasi-optical techniques at millimeter and submillimeter wavelengths," in *Infrared and Millimeter Waves*, vol. 6, K. J. Button, Ed. New York: Academic, 1982, ch. 5.

Reuven Shavit (M'82-SM'90), for a photograph and biography please see page 484 of the April 1991 issue of the TRANSACTIONS.

Adam P. Smolski, for a photograph and biography please see page 484 of the April 1991 issue of this TRANSACTIONS.

Eric Michielssen, for a photograph and biography please see page 490 of the April 1991 issue of this TRANSACTIONS.

Raj Mittra (S'54-M'57-SM'69-F'71), for a photograph and biography please see page 545 of the May 1989 issue of this TRANSACTIONS.